Noninvasive gene targeting to the brain

Ningya Shi and William M. Pardridge*

Department of Medicine, University of California School of Medicine, Los Angeles, CA 90095-1682

Communicated by M. Frederick Hawthorne, University of California, Los Angeles, CA, April 25, 2000 (received for review March 1, 2000)

Gene therapy of the brain is hindered by the presence of the blood–brain barrier (BBB), which prevents the brain uptake of bloodborne gene formulations. Exogenous genes have been expressed in the brain after invasive routes of administration, such as craniotomy or intracarotid arterial infusion of noxious agents causing BBB disruption. The present studies describe the expression of an exogenous gene in brain after noninvasive i.v. administration of a 6- to 7-kb expression plasmid encoding either luciferase or β-galactosidase packaged in the interior of neutral pegylated immunoliposomes. The latter are conjugated with the OX26 mAb to the rat transferrin receptor, which enables targeting of the plasmid DNA to the brain via the endogenous BBB transferrin receptor. Unlike cationic liposomes, this neutral liposome formulation is stable in blood and does not result in selective entrapment in the lung. Luciferase gene expression in the brain peaks at 48 h after a single i.v. administration of 10 μg of plasmid DNA per adult rat, a dose that is 30- to 100-fold lower than that used for gene expression in rodents with cationic liposomes. β-Galactosidase histochemistry demonstrated gene expression throughout the central nervous system, including neurons, choroid plexus epithelium, and the brain microvasculature. In conclusion, widespread gene expression in the brain can be achieved by using a formulation that does not employ viruses or cationic liposomes, but instead uses endogenous receptor-mediated transport pathways at the BBB.

blood–brain barrier | transferrin receptor | monoclonal antibody | gene therapy

The expression of exogenously administered genes in brain has been achieved *in vivo* with either viral vectors or cationic liposomes (1–4). However, in either case, highly invasive routes of administration were used, owing to the failure of gene medicines to cross the brain capillary wall, which forms the blood–brain barrier (BBB) *in vivo*. The existence of the BBB necessitates the administration of the exogenous gene, either intracerebrally via craniotomy (1), or by the intracarotid arterial infusion of noxious agents that cause BBB disruption (4).

Human gene therapy of the brain will likely require repeated administration of the gene medicine. Therefore, it would be advantageous to administer the gene by a route that is no more invasive than a simple i.v. injection. With this approach, the gene therapeutic is delivered through the BBB by targeting the gene medicine to the brain via endogenous BBB transport systems (5). Peptidomimetic mAbs that bind endogenous transport systems within the BBB, such as the transferrin receptor (TfR) or insulin receptor, have been used in previous studies for targeting neuropeptides or antisense agents through the BBB *in vivo* (5). However, using endogenous BBB transport systems to target gene medicines noninvasively to the brain also requires the development of a suitable formulation of the gene therapeutic that is stable in the bloodstream. Cationic liposome/DNA complexes have been used for *in vivo* gene expression, but these formulations aggregate extensively in saline solution (6–11). This aggregation results in selective gene expression in the lung, with little expression in peripheral tissues (12–14) and no expression in brain after i.v. administration of the cationic liposome/DNA complex (12). The DNA plasmid could be conjugated to the peptidomimetic mAb via a cationic polylysine bridge (15–17). However, electrostatic interactions between DNA and polycations my not be stable in blood, and highly polycationic proteins such as histone or polylysine exert toxic effects at the BBB and cause generalized BBB permeability changes *in vivo* (18). A third approach is to incorporate the plasmid DNA within the interior of conventional neutral liposomes. The stability of the liposome in the circulation may be enhanced by incorporating several thousand polyethylene glycol (PEG) strands on the surface of the liposome, which prevent rapid uptake by the reticulo-endothelial system, and the PEG optimizes the plasma bioavailability of the liposome. The presence of the PEG strands also provides a site for conjugation of peptidomimetic mAbs, which then target the pegylated immunoliposomes through the BBB *in vivo* (19).

The present studies describe a novel formulation of an exogenous plasmid DNA, wherein either a β-galactosidase or a luciferase expression plasmid, driven by the SV40 promoter, is incorporated in the interior of neutral liposomes that are pegylated with PEG of 2000 Daltons molecular mass, designated PEG 2000. Approximately 40 of the PEG strands per liposome are tethered with the OX26 murine mAb to the rat transferrin receptor. The OX26 mAb, or transferrin, undergo receptor-mediated transcytosis through the BBB *in vivo*. This property of a peptidomimetic mAb, such as OX26, enables brain targeting of the pegylated immunoliposomes by triggering transport into brain via the BBB TfR.

Experimental Procedures

Materials. POPC (1-palmitoyl-2-oleoyl-*sn*-glycerol-3-phosphocholine) and DDAB (didodecyldimethylammonium bromide) were purchased from Avanti Polar Lipids. Distearoylphosphatidylethanolamine (DSPE)-PEG 2000 was obtained from Shearwater Polymers (Huntsville, AL). DSPE-PEG 2000-maleimide was custom synthesized by Shearwater Polymers. [α-^{32}P]dCTP (800 Ci/mmol) was from NEN Research Products. ^{125}NaI and *N*-succinimidyl[2,3-^{3}H]propionate (^{3}H-NSP) was from Amersham Life Science. The nick translation system was purchased from GIBCO/BRL. Pancreatic DNase I (from bovine pancreases), with a specific activity of 2000 Kunitz units/mg was purchased from Sigma. Luciferase reagent, recombinant luciferase, the 6.8-kb pSV-β-galactosidase plasmid, and exonuclease III were obtained from Promega. Protein G Sepharose CL-4B was from Amersham Pharmacia. Mouse myeloma ascites IgG2a (κ) was from Cappel. Centriprep-30 (molecular weight cutoff: 30,000) concentrator was obtained from Amicon. Male Sprague–Dawley rats (weighing from 200–250 g) were obtained from Harlan–Sprague–Dawley.

Abbreviations: BBB, blood–brain barrier; TfR, transferrin receptor; PEG, polyethyleneglycol; TCA, trichloroacetic acid; HIR, human insulin receptor; DSPE, distearoylphosphatidylethanolamine.

*To whom reprint requests should be addressed. E-mail: wpardridge@mednet.ucla.edu.

The publication costs of this article were defrayed in part by page charge payment. This article must therefore be hereby marked "*advertisement*" in accordance with 18 U.S.C. §1734 solely to indicate this fact.

Article published online before print: *Proc. Natl. Acad. Sci. USA*, 10.1073/pnas.130187497. Article and publication date are at www.pnas.org/cgi/doi/10.1073/pnas.130187497

Plasmid Production. The 5.8-kb plasmid, pGL_2, encoding for the firefly *Photinus pyralis* luciferase gene, or the 6.8-kb pSV-β-galactosidase plasmid, both under the influence of the SV40 promoter, were obtained from Promega. The plasmids were amplified in the JM109 strain of *Escherichia coli*. DNA was extracted by using alkaline lysis method and purified by precipitation with isopropanol, using QIAfilter Plasmid Maxi kit (Qiagen, Chatsworth, CA). DNA was measured by UV absorption at 260 nm and dissolved in TE buffer [10 mM Tris/1 mM EDTA (pH 8.0)]. Linearized DNA was obtained by digestion with *Bam*HI. Its size was confirmed by 0.8% agarose gel electrophoresis and ethidium bromide staining.

DNA Radiolabeling. Supercoiled DNA was labeled with [α-^{32}P]dCTP by the nick translation method (Nick Translation System, Promega), using DNA polymerase I and DNase I. Unincorporated nucleotide was removed by a G25 Sephadex column (Roche Molecular Biochemicals). The specific activity of the labeled probe is 5×10^6 cpm/μg.

The linearized plasmid was ^{32}P-radiolabeled at both 5′ and 3′ ends with T4 polymerase and purified with a Sephadex G-25 spin column to a trichloroacetic acid (TCA) precipitability of 98%. This material was analyzed with 0.8% agarose gel electrophoresis and film autoradiography and migrated as a single band of 5.8 kb with no low molecular weight radiolabeled impurities.

The ^{32}P-linearized plasmid was used in the pharmacokinetic experiments. The ^{32}P-supercoil plasmid was used as a tracer to measure the incorporation of the unlabeled supercoil plasmid in the liposomes.

Pegylated Liposome Synthesis and Plasmid DNA Encapsulation. POPC (19.2 μmol), DDAB (0.2 μmol), DSPE-PEG 2000 (0.6 μmol), and DSPE-PEG 2000-maleimide (30 nmol) were dissolved in chloroform/methanol (2:1, vol:vol) followed by evaporation. The lipids were dispersed in 1 ml 0.05 M Tris·HCl buffer (pH = 8.0) and sonicated for 10 min (20). Supercoiled DNA (100 μg) and 1 μCi ^{32}P[DNA] were added to the lipids. The liposome/DNA dispersion was evaporated to a final concentration of 200 mM at a volume of 100 μl. The dispersion was frozen in ethanol/dry ice for 4–5 min and thawed at 40°C for 1–2 min, and this freeze-thaw cycle was repeated 10 times. The liposome dispersion was diluted to a lipid concentration of 40 mM, followed by extrusion 10 times each through two stacks each of 400-nm, 200-nm, 100-nm, and 50-nm pore size polycarbonate membranes, by using a hand held extruder (Avestin, Ottawa), as described previously (19). The mean vesicle diameters were determined by quasielastic light scattering by using a Microtrac Ultrafine Particle Analyzer (Leeds–Northrup, St. Petersburg, FL), as described previously (19).

The plasmid absorbed to the exterior of the liposomes was removed by nuclease digestion (20). For digestion of the unencapsulated DNA, 5 units of pancreatic endonuclease I and 5 units of exonuclease III were added in 5 mM $MgCl_2$ and 0.1 mM DTT to the liposome/DNA mixture after extrusion. After incubation at 37°C for 1 h, the reaction was stopped by adding 7 mM EDTA. The extent to which the nuclease digestion removed the exteriorized plasmid DNA was determined by agarose gel electrophoresis and ethidium bromide staining of aliquots taken before and after nuclease treatment.

Conjugation of OX26 mAb or Mouse IgG2a to the Pegylated Liposome/DNA. The anti-rat transferrin receptor OX26 mAb was harvested from serum-free OX26 hybridoma-conditioned media as described (21). OX26, as well as the isotype control, mouse IgG2a, were purified by protein G Sepharose affinity chromatography (21). OX26 was radiolabeled with *N*-succinimidyl[2,3-^{3}H]propionate (^{3}H-NSP) as described previously (22). The ^{3}H[OX26] had a specific activity of 0.13 μCi/μg and a TCA precipitability of 95%.

The OX26 or mouse IgG2a (1.5 mg, 10 nmol) was thiolated by using a 40:1 molar excess of 2-iminothiolane (Traut's reagent), as described previously (19). The number of OX26 molecules conjugated per liposome was calculated from the total OX26 cpm in the liposome pool and the specific activity of the labeled OX26 mAb, assuming 100,000 lipid molecules per liposome, as described previously (19). The final percentage entrapment of the 100 μg of pGL2 in the liposome preparation was computed from the ^{32}P radioactivity and was typically 30% or 30 μg of plasmid DNA. This preparation was then administered to three rats at a dose of 10 μg of plasmid DNA per rat for luciferase gene expression measurements.

Pharmacokinetics. A pharmacokinetic study was performed in ketamine/xylazine-anesthetized male Sprague–Dawley rats, as described previously (19). The ^{32}P[pGL2] (1 uCi) was injected in one of the following three formulations: (*i*) naked DNA, (*ii*) DNA encapsulated in pegylated liposomes without Ab attached, or (*iii*) DNA encapsulated in pegylated liposomes with OX26 mAb conjugated to the PEG strands.

Luciferase Gene Expression *in Vivo*. The pegylated liposome/luciferase DNA that was conjugated with either OX26 mAb or mouse IgG2a was injected i.v. into anesthetized rats at a dose of 10 μg of pGL2 DNA per rat. Rats were killed at 24, 48, or 72 h after injection. The brain, heart, kidney, spleen, liver, and lung tissues were homogenized in 4 vol of lysis buffer containing 0.1 M potassium phosphate buffer (pH 7.8), 1% Triton X-100, 1 mM DTT, and 2 mM EDTA by using a Polytron (Kinematica, Lucerne, Switzerland) homogenizer. The homogenate was centrifuged at 14,000 rpm for 10 min at 4°C. The supernatant was used for measurement of tissue luciferase activity with a Luminometer (Biolumat LB 9507, Berthold, Nashua, NH); 100 μl of reconstituted luciferase substrate was added to 20 μl of tissue extract. Peak light emission was measured for 10 sec at 20°C, and recorded as relative light units, as described previously (23). The background level was determined by measuring a sample containing only lysis buffer. The protein concentration in the tissue extract was determined with the bicinchoninic acid (BCA) protein assay reagent (Pierce).

***β*-Galactosidase Gene Expression *in Vivo*.** The pegylated immunoliposome/β-galactosidase DNA was prepared exactly as described above with the OX26 mAb, and injected i.v. in rats as described above at a dose of 50 μg of plasmid DNA per 0.25 kg adult rat. At 48 h later, the brain and liver were removed and rapidly frozen in powdered dry ice, dipped in Tissue-Tek (Fisher Scientific) OCT embedding medium, and 15-μm frozen sections were prepared on a Bright cryostat. The sections were fixed for 5 min at room temperature in 0.5% glutaraldehyde in 0.1 M NaH_2PO_4, and stored at −70°, until β-galactosidase histochemistry with 5-bromo4-chloro-3-indoyl-β-D-galactoside (X-Gal, Promega), as described by the manufacturer. Slides were developed overnight at 37°C, and some slides were counterstained with Mayer's hematoxylin. The slides were photographed or scanned with a 1200 dpi UMAX flatbed scanner with transilluminator, and cropped with Adobe (Adobe Systems, Mountain View, CA) PHOTOSHOP 5.5 with a G4 Power Macintosh.

Results

The structure of the pegylated immunoliposome carrying the pGL2 luciferase plasmid within the interior of the liposome is shown in Fig. 1*A*. The mean diameter of the pegylated immunoliposomes carrying the pGL2 plasmid in the interior is 73 nm (Fig. 1*B*). The nuclease treatment removes any plasmid DNA bound to the exterior of the pegylated liposome (see *Experi-*

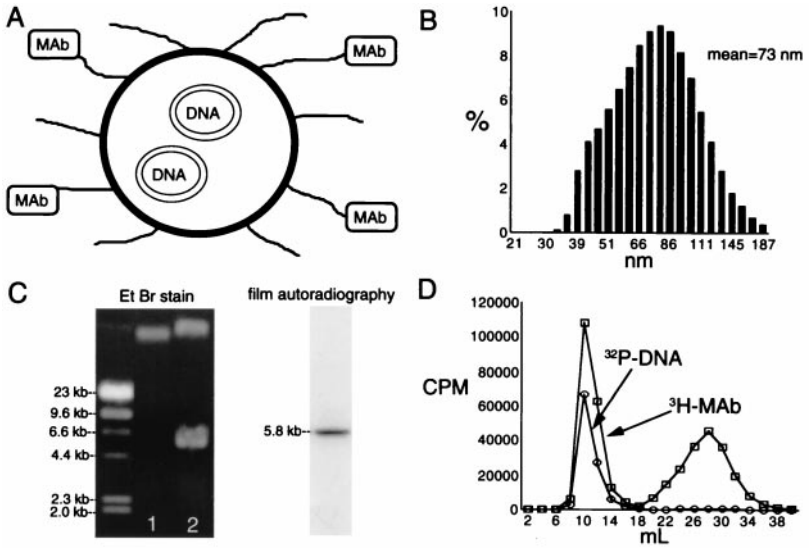

Fig. 1. (A) Scheme showing plasmid (DNA) encapsulated in pegylated immunoliposomes constructed from neutral lipids. There are approximately 3000 strands of polyethylene glycol of 2000 Da molecular mass, designated PEG 2000, attached to the liposome surface, and about 1% of the PEG strands is conjugated with an mAb to a BBB receptor. (*B*) The mean diameter of the pegylated liposomes encapsulating the pGL2 plasmid DNA is 73 nm. (*C*) Liposomes before (lane 2) and after (lane 1) DNase 1/exonuclease III treatment were resolved with 0.8% agarose gel electrophoresis followed by ethidium bromide (Et Br) staining. DNA molecular weight size standards are shown in the left hand side. Approximately 50% of the DNA associated with the pegylated liposome was bound to the exterior of the liposome (lane 2), and the exteriorized DNA was quantitatively removed by the nuclease treatment (lane 1). A trace amount of the pGL2 plasmid was radiolabeled with ^{32}P, and film autoradiography of the gel showed a single 5.8-kb band with no low molecular weight radiolabeled DNA. (*D*) The conjugation of the OX26 mAb to the pegylated liposomes carrying the encapsulated pGL2 plasmid DNA after nuclease digestion is demonstrated by Sepharose CL-4B gel filtration chromatography. A trace amount of the encapsulated pGL2 plasmid DNA was labeled with ^{32}P, and a trace amount of the OX26 mAb was radiolabeled with ^{3}H. The study shows the comigration of the conjugated OX26 mAb and the encapsulated pGL2 plasmid DNA.

mental Procedures), and ethidium bromide staining after agarose gel electrophoresis demonstrates complete removal of any exterior bound plasmid from the preparation (Fig. 1*C*, lane 1). When the pGL2 plasmid DNA was radiolabeled with ^{32}P before incorporation into the liposomes, only the 5.8-kb pGL2 plasmid was detected, and no low molecular weight forms of DNA were observed (Fig. 1*C*, film autoradiography). The covalent conjugation of the OX26 mAb to the tips of the PEG strands on the pegylated immunoliposome was monitored by Sepharose CL-4B gel filtration chromatography (Fig. 1*D*). These studies show comigration of the ^{32}P[pGL2] incorporated in the interior of the liposome with the ^{3}H-labeled OX26 mAb attached to the PEG strands. Based on the specific activity of the OX26, it was calculated that this preparation of pegylated immunoliposome contained 39 molecules of OX26 mAb conjugated to the individual liposome.

The pharmacokinetic studies were performed with the linearized pGL2 plasmid DNA, which was end labeled with ^{32}P. The naked DNA was rapidly removed from the plasma with a clearance (CL) of 4.1 ± 0.5 ml/min per kg and a systemic volume of distribution of 514 ± 243 ml/kg. The CL of the DNA was reduced more than 4-fold to 0.95 ± 0.05 ml/min per kg when the DNA was incorporated in the interior of pegylated liposomes carrying no OX26 mAb (Fig. 2 *Left*). The systemic clearance increased to 2.3 ± 0.2 ml/min per kg when the OX26 mAb was tethered to the tip of the PEG tail of the liposome.

The attachment of the OX26 mAb to the tip of the pegylated liposome carrying the DNA exerted minor increases in tissue uptake in kidney or heart, moderate increases in liver, and a marked increase in the brain uptake of the pegylated immunoliposome (Fig. 3). The brain uptake of the pegylated immunoliposome carrying the plasmid DNA is comparable to the brain uptake of a neuroactive small molecule such as morphine (24).

The luciferase gene expression in brain and peripheral tissues was examined in rats administered 10 μg of plasmid DNA per rat. Although there was minimal targeting of the luciferase gene in the heart or kidney, the luciferase gene expression in brain was comparable to that of lung or spleen and peaked at 48 h after i.v. administration (Fig. 4). The peak luciferase gene expression in liver was approximately 6-fold higher than in brain, owing to the abundant expression of TfR on hepatocyte plasma membranes. For control studies, pegylated immunoliposomes were prepared, except that mouse IgG2a, which is the isotype control of OX26, was conjugated to the pegylated liposomes in lieu of the OX26 mAb. The mouse IgG2a-pegylated immunoliposome/pGL2

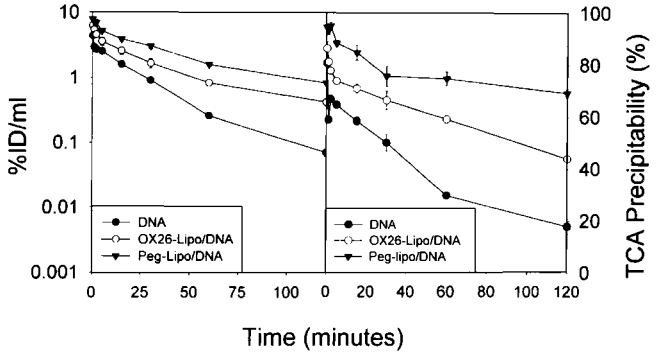

Fig. 2. (left) The percentage of injected dose (ID) per ml plasma that is precipitated by TCA is plotted vs. the time after i.v. injection of the ^{32}P DNA in anesthetized rats for up to 120 min. The DNA was injected 1 of 3 formulations: (*i*) ''naked'' DNA (DNA), (*ii*) pGL2 plasmid DNA encapsulated within the interior of nuclease-treated OX26-pegylated immunoliposomes (OX26-Lipo/DNA), and (*iii*) pGL2 plasmid DNA encapsulated in the interior of nuclease-treated pegylated liposomes without OX26 mAb attached (Peg-Lipo/DNA) (*Right*). The percentage of plasma radioactivity that is precipitated by TCA is shown. Data mean are ± SE (n = 3 rats/group).

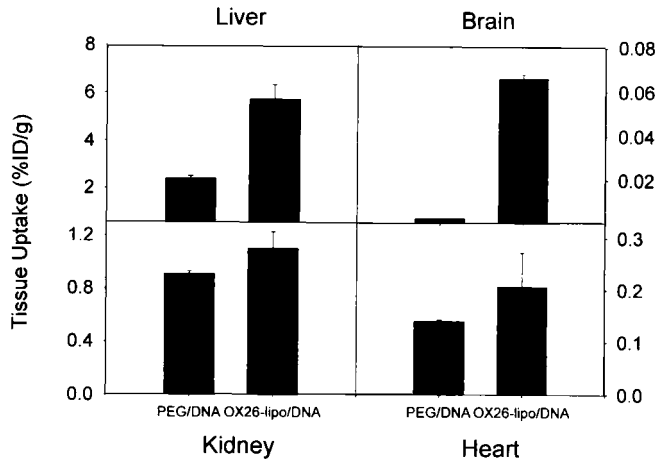

Fig. 3. The tissue uptake, expressed as percentage injected dose (ID) per gram of tissue, for liver, brain, kidney, or heart is shown at 120 min after i.v. injection of the encapsulated ^{32}P pGL2 plasmid DNA incorporated in either pegylated liposomes without Ab attached (PEG/DNA) or within the OX26 pegylated immunoliposomes (OX26-Lipo/DNA). Data are mean ± SE (n = 3 rats/group).

DNA complex was injected i.v. into anesthetized rats; the dose of pGL2 plasmid DNA was 10 μg per rat, or 40 μg/kg. However, there was no measurable luciferase expression in brain or in any of the other organs at 48 h after i.v. administration. This control experiment was repeated three times, and the luciferase activity was below the limits of detection in all samples.

The β-galactosidase histochemistry is shown in Fig. 5. The brain expresses the β-galactosidase gene widely as seen at low magnification (Fig. 5*A*), whereas no β-galactosidase activity is observed in the control brain (Fig. 5*B*). Pyramidal neurons of the CA1-CA3 sectors of the hippocampus are clearly visualized as are the choroid plexi in both lateral ventricles and in both the dorsal horn and the mamillary recess of the third ventricle (Fig. 5*A*). The paired supraoptic nuclei of the hypothalamus at the base of the brain are viewed at low magnification (Fig. 5*A*). At higher magnification, the microvasculature of brain parenchyma (Fig. 5*C*), the choroid plexus epithelium (Fig. 5*D*), and thalamic nuclei (Fig. 5*E*) showed β-galactosidase gene expression. Lower levels of gene expression in neurons throughout the brain were also visualized. Gene expression was detected histochemically throughout the liver in a periportal pattern, and gene expression was localized to hepatocytes, as shown in Fig. 5*F*. The high magnification view shows a punctate deposition of enzyme product throughout the liver cell.

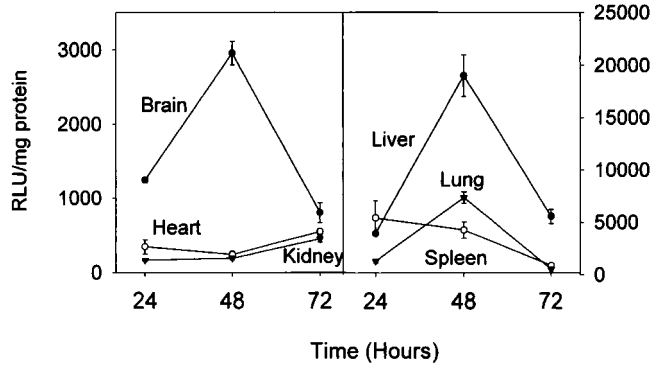

Fig. 4. The organ luciferase activity, expressed as relative light units (RLU) per mg of tissue protein, is shown for brain, heart, kidney, liver, lung, and spleen at 24, 48, and 72 h after injection of the pGL2 plasmid DNA encapsulated in pegylated immunoliposomes that were conjugated with the OX26 mAb. Data are mean ± SE (n = 3 rats/group).

Discussion

These studies are consistent with the following conclusions. First, a formulation for gene therapy is described that brings together liposome technology, pegylation technology, BBB targeting technology, and plasmid-based therapeutic genes (Fig. 1*A*). Second, the use of the pegylated liposome results in an increase in the plasma bioavailability of the plasmid DNA incorporated within the interior of the pegylated immunoliposome and also results in an increased plasmid stability (Fig. 2). Third, with this formulation, it is possible to achieve expression of an exogenous gene in the brain after noninvasive i.v. administration (Figs. 4 and 5). It is also possible to achieve, in parallel, gene expression in other organs, such as liver, that also express high levels of the receptor targeted by the peptidomimetic mAb, in this case, the TfR (Figs. 4 and 5).

The formulation of the plasmid gene incorporated within a pegylated immunoliposome is shown in Fig. 1*A*, and this formulation has features distinct from cationic liposome/DNA complexes. The latter form 80- to 100-nm small unilamellar vesicles when formulated in water, but rapidly aggregate in physiological saline into structures $\geq$1 μm (11, 14). The ability of cationic liposome/DNA complexes to transfect cells in tissue culture is a function of the aggregation properties of this formulation (10). The complex aggregates in saline solution, which then triggers phagocytosis, not endocytosis, by the cultured cells (7). Therefore, it is difficult to target cationic liposome/DNA complexes to cells by using receptor-mediated endocytosis systems. The pegylated immunoliposome described in Fig. 1*A* also has advantages over viral formulations. The pegylated immunoliposome comprises normal cellular constituents that do not trigger the immune system. In contrast, viral vectors can be toxic to the brain. The intracerebral injection of adenovirus into the brain causes inflammation and an increase in expression of the class I multiple histocompatibility Ag in brain (25).

The pegylation of the liposome surface serves the dual purpose of (*i*) prolonging the plasma residence time and increasing the plasma stability (Fig. 2), and (*ii*) tethering the tip of the PEG tail with a brain-targeting vector that undergoes receptor-mediated transcytosis through the BBB. Placement of a targeting Ab at the tip of the PEG tail, rather than the surface of the liposome, removes any steric hindrance in binding of the mAb to its cognate receptor on the BBB that might be caused by the PEG strands (19). The number of surface lipid molecules of the liposome that are pegylated constitute 3% of the lipid (see *Experimental Procedures*). Because a 100-nm liposome contains approximately 100,000 lipid molecules on the surface (19), there are approximately 3000 PEG strands per individual liposome. Because there are 30–40 OX26 mAb molecules attached per individual liposome, approximately 1% of the PEG strands have the Ab conjugated to the tip of the strand. Cationic liposome/DNA complexes have been pegylated (26). However, this pegylation does not eliminate the avid uptake of the cationic liposome by the lung (26). After i.v. injection of cationic liposomes, the gene expression in the lung is more than 100-fold greater than gene expression in other organs, such as liver, with no gene expression in brain (12). The pulmonary circulation is the first capillary bed that a molecule passes through after i.v. administration, and cationic liposome/DNA complexes that aggregate immediately in the saline of plasma will promptly deposit in the lung microvasculature (12–14). In addition, cationic liposomes may bind to heparin proteoglycans on the pulmonary endothelial surface (27). In contrast, the formulation

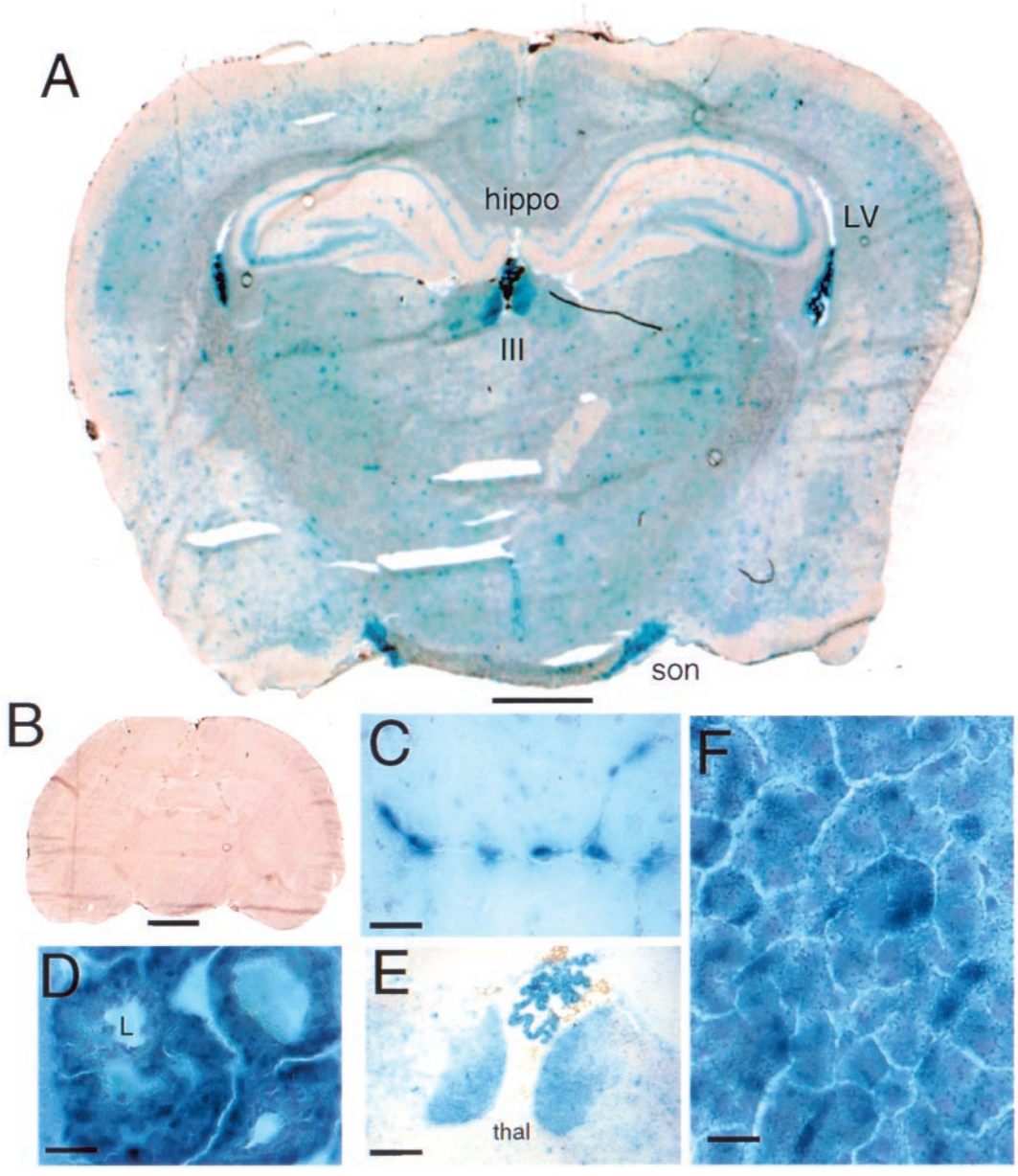

Fig. 5. β-galactosidase histochemistry in brain (*A–E*) and liver (*F*) at 48 h after i.v. injection of the β-galactosidase gene packaged inside the OX26 pegylated immunoliposome (*B–F*). The control brain from rats receiving no gene administration is shown in *B*. Magnification bars = 1.5 mm (*A*), 2.2 mm (*B*), 57 μm (*C*), 23 μm (*D*), 230 μm (*E*), and 15 μm (*F*). *A* and *B* were not counterstained. The lateral ventricles (LV), third ventricle (III), left or right hippocampus (hippo), and hypothalamic supraoptic nuclei (son) are labeled in *A*. *C* shows punctate gene expression in intraparenchymal capillaries and may represent gene expression in either endothelium or microvascular pericytes. (*D*) Gene expression in the epithelium of the choroid plexus. The lumen (L) of a capillary of the choroid plexus is shown and demonstrates the absence of β-galactosidase enzyme activity in the plasma compartment. (*E*) The thalamic (thal) nuclei below the choroid plexus of the third ventricle, which is also visible in *A*. (*F*) Abundant gene expression in hepatocytes; this high magnification shows a speckled pattern, suggesting localization of the β-galactosidase enzyme within the liver cell endoplasmic reticulum.

described in Fig. 1 does not result in preferential gene expression in the pulmonary circulation compared with liver or other tissues (Fig. 4). There is gene expression in the lung that is about one-fourth the gene expression in the liver, and the lung gene expression arises from targeting by the OX26 mAb to TfR present in lung. Previous studies show that anti-TfR mAbs are targeted to the lung *in vivo* to a greater extent than other peripheral tissues, such as kidney or heart (28), and these previous findings are paralleled by the tissue-specific gene expression observed with pegylated immunoliposomes (Fig. 4).

The measurement of organ radioactivity (Fig. 3) does not accurately reflect the organ targeting of the gene, if there is significant uptake of ^{32}P-labeled metabolites released after organ degradation of the ^{32}P-plasmid DNA. As shown by the decreasing TCA precipitability of the plasma radioactivity (Fig. 2), there is significant degradation of the plasmid *in vivo*, which results in the release to blood of TCA-soluble metabolites such as [^{32}P]phosphate. The latter is rapidly taken up by tissues such as liver or kidney, and much less so by organs such as brain. The uptake of phosphate accounts for the relatively high tissue radioactivity of the liver after administration of the labeled DNA packaged in pegylated liposomes without TfR mAb attached (Fig. 3).

The targeting specificity of the pegylated immunoliposome is strictly a function of the targeting moiety attached to the tip of the PEG strands (Fig. 1*A*). The replacement of the TfR mAb with an IgG2a isotype control results in no organ expression of the luciferase gene (see *Results*). The expression of the luciferase trans gene in brain peaks at 48 h after i.v. administration (Fig. 4). This level of gene expression is comparable to that found in liver after the i.v. injection in rats of plasmid DNA absorbed to polylysine, which was then conjugated to carbohydrate moieties that target the asialoglycoprotein receptor on the hepatocyte plasma membrane (17). However, in this latter study, 300 μg of plasmid DNA was i.v. administered to adult rats (17). This dose is 30-fold greater than the dose used in the present studies, which is 10 μg of plasmid DNA per adult rat, or 40 μg of plasmid DNA per kg body weight. In contrast, the dose of cationic liposomes/DNA complexes administered to mice *in vivo* to generate gene expression in lung ranges from 1000–4000 μg of plasmid DNA per kg body weight (13, 14, 26, 29, 30).

The β-galactosidase histochemistry shows that the gene is widely expressed throughout the brain, including neurons, as shown for the hippocampus (Fig. 5*A*) and the thalamus (Fig. 5*E*). Therefore, the pegylated immunoliposome carrying the transgene traverses both the BBB and the neuronal cell membrane. The uptake into brain cells occurs because the targeting moiety mediates both the transcytosis through the BBB and the endocytosis of the complex into brain cells. These pathways are accessed owing to expression of the TfR both on the brain capillary endothelium (31), which forms the BBB *in vivo*, and on the plasma membrane of brain cells (32). The liposomes may fuse with endosomal membranes within brain cells, which allows for extrusion of the plasmid DNA into the cytosolic compartment, where the DNA can then move into the nuclear space. Based on the β-galactosidase histochemistry for liver, the β-galactosidase protein is targeted to the endoplasmic reticulum, which is suggested by the deposition of enzyme product on a tubulovesicular network within the cytosol of the hepatocyte (Fig. 5*F*).

In summary, these studies demonstrate that it is possible using brain targeting technology to achieve widespread expression of an exogenous gene in the brain after noninvasive i.v. administration. Replacement of the SV40 promoter and 3-untranslated region (UTR) parts of the plasmid with tissue- and gene-specific promoters and 3-UTR elements should enable brain-, region- and even cell-specific gene expression. For example, the lack of significant gene expression in the outer rim of the brain cortex (Fig. 5) suggests that the SV40 promoter is not activated in this region. The insertion of different UTR elements results in a 50-fold increase in luciferase gene expression in brain at 72 h, relative to the activity shown in Fig. 4 (unpublished data). The present approach to gene therapy could be used in humans by changing the targeting moiety of the formulation (Fig. 1*A*) to enable targeting the human insulin receptor (HIR). An mAb that targets the HIR (33) is nearly 10 times more active in primates than is the anti-TfR mAb (5). Chimeric forms of the HIR mAb have been recently described, and the genetically engineered chimeric HIR mAb has transport properties at the primate or human BBB that are identical to that of the original murine Ab (34). The insulin receptor is also widely distributed on brain cells (35), so the HIR mAb would direct the gene formulation through both barriers in brain, the BBB, and the brain–cell membrane.

Daniel Jeong skillfully prepared the manuscript. We are indebted to Dr. Ruben J. Boado for valuable discussions.

1. Culver, K. W., Ram, Z., Wallbridge, S., Ishii, H., Oldfield, E. H. & Blaese, R. M. (1992) *Science* **256,** 1550–1552.
2. Suhr, S. T. & Gage, F. H. (1993) *Arch. Neurol.* **50,** 1252–1268.
3. Martin, J. B. (1995) *Trends Biotechnol.* **13,** 28–35.
4. Nilaver, G., Muldoon, L. L., Kroll, R. A., Pagel, M. A., Breakefield, X. O., Davidson, B. L. & Neuwelt, E. A. (1995) *Proc. Natl. Acad. Sci. USA* **92,** 9829–9833.
5. Pardridge, W. M. (1997) *J. Cereb. Blood Flow Metabol.* **17,** 713–731.
6. Reimer, D. L., Zhang, Y., Kong, S., Wheeler, J. J., Graham, R. W. & Bally, M. B. (1995) *Biochemistry* **34,** 12877–12883.
7. Matsui, H., Johnson, L. G., Randell, S. H. & Boucher, R. C. (1997) *J. Biol. Chem.* **272,** 1117–1126.
8. Mahato, R. I., Rolland, A. & Tomlinson, E. (1997) *Pharm. Res.* **14,** 853–859.
9. Huang, L. & Li, S. (1997) *Nat. Biotechnol.* **15,** 620–621.
10. Niidome, T., Ohmori, N., Ichinose, A., Wada, A., Mihara, H., Hirayama, T. & Aoyagi, H. (1997) *J. Biol. Chem.* **272,** 15307–15312.
11. Plank, C., Tang, M. X., Wolfe, A. R. & Szoka, F. C. (1999) *Hum. Gene Ther.* **10,** 319–332.
12. Osaka, G., Carey, K., Cuthbertson, A., Godowski, P., Patapoff, T., Ryan, A., Gadek, T. & Mordenti, J. (1996) *J. Pharm. Sci.* **85,** 612–618.
13. Hofland, H. E. J., Nagy, D., Liu, J.-J., Spratt, K., Lee, Y. L., Danos, O. & Sullivan, S. M. (1997) *Pharm. Res.* **14,** 742–749.
14. Song, Y. K., Liu, F., Chu, S. & Liu, D. (1997) *Hum. Gene Ther.* **8,** 1585–1594.
15. Wu, G. Y. & Wu, C. H. (1987) *J. Biol. Chem.* **262,** 4429–4432.
16. Chowdhury, N. R., Wu, C. H., Wu, G. Y., Yerneni, P. C., Bommineni, V. R. & Chowdhury, J. R. (1993) *J. Biol. Chem.* **268,** 11265–11271.
17. Perales, J. C., Grossmann, G. A., Molas, M., Liu, G., Ferkol, T., Harpst, J., Oda, H. & Hanson, R. W. (1997) *J. Biol. Chem.* **272,** 7398–7407.
18. Pardridge, W. M., Triguero, D. & Buciak, J. B. (1989) *J. Pharmacol. Exp. Ther.* **251,** 821–826.
19. Huwyler, J., Wu, D. & Pardridge, W. M. (1996) *Proc. Natl. Acad. Sci. USA* **93,** 14164–14169.
20. Monnard, P.-A., Oberholzer, T. & Luisi, P. (1997) *Biochim. Biophys. Acta* **1329,** 39–50.
21. Kang, Y.-S. & Pardridge, W. M. (1994) *J. Pharmacol. Exp. Ther.* **269,** 344–350.
22. Pardridge, W. M., Buciak, J. L. & Yoshikawa, T. (1992) *J. Pharmacol. Exp. Ther.* **261,** 1175–1180.
23. Dwyer, K. J., Boado, R. J. & Pardridge, W. M. (1996) *J. Neurochem.* **66,** 449–458.
24. Wu, D., Kang, Y.-S., Bickel, U. & Pardridge, W. M. (1997) *Drug Metab. Disp.* **25,** 768–771.
25. Wood, M. J. A., Charlton, H. M., Wood, K. J., Kajiwara, K. & Byrnes, A. P. (1996) *Trends Neurosci.* **19,** 497–501.
26. Hong, K., Zheng, W., Baker, A. & Papahadjopoulos, D. (1997) *FEBS Lett.* **400,** 233–237.
27. Mounkes, L. C., Zhong, W., Ciperes-Palacin, G., Heath, T. D. & Debs, R. J. (1998) *J. Biol. Chem.* **273,** 26164–26170.
28. Lee, H. J., Engelhardt, B., Lesley, J., Bickel, U. & Pardridge, W. M. (2000) *J. Pharmacol. Exp. Ther.* **292,** 1048–1052.
29. Barron, L. G., Uyechi, L. S. & Szoka, F. C. (1999) *Gene Ther.* **6,** 1179–1183.
30. Zhu, N., Liggitt, D., Liu, Y. & Debs, R. (1993) *Science* **261,** 209–212.
31. Huwyler, J. & Pardridge, W. M. (1998) *J. Neurochem.* **70,** 883–886.
32. Mash, D. C., Pablo, J., Flynn, D. D., Efange, S. M. & Weinger, W. J. (1990) *J. Neurochem.* **55,** 1972–1979.
33. Pardridge, W. M., Kang, Y.-S., Buciak, J. L. & Yang, J. (1995) *Pharm. Res.* **12,** 807–816.
34. Coloma, M. J., Lee, H. J., Kurihara, A., Landaw, E. M., Boado, R. J., Morrison, S. L. & Pardridge, W. M. (2000) *Pharm. Res.* **17,** 266–274.
35. Zhao, W., Chen, H., Xu, H., Moore, E., Meiri, N., Quon, M. J. & Alkon, D. L. (1999) *J. Biol. Chem.* **274,** 34893–34902.